Iranian Journal of Materials Forming 13 (2) (2026) 47-58

Online ISSN: 2383-0042

IJMF

Iranian Journal of Materials Forming

Journal Homepage: http://ijmf.shirazu.ac.ir

Research Article

Investigation of the Superplastic Behavior of 1050 Aluminum Strip Processed by the ECAP-Pull Method

Amir Taher and Peyman Mashhadi Keshtiban*

Faculty of Mechanical Engineering,Urmia University of Technology, Urmia, Iran

ARTICLE INFO

Article history:

Received: 1 November 2025
Reviewed: 22 November 2025
Revised: 16 December 2025
Accepted: 20 December 2025

Keywords:

Superplastic behavior
Severe plastic deformation (SPD)
ECAP-Pull

Please cite this article as:

Taher, A., & Mashhadi Keshtiban, P. (2026). Investigation of the superplastic behavior of 1050 aluminum strip processed by the ECAP-pull method. *Iranian Journal of Materials Forming*, *13*(2), 47-58. https://doi.org/10.22099/IJMF.2026.54698.1358

ABSTRACT

This study introduces a novel, energy-efficient severe plastic deformation (SPD) technique termed equal channel angular pulling (ECAP-Pull). This method replaces the conventional pressing action with a tensile force, enabling the continuous processing of long strips. Commercial purity AA1050 aluminum strips were successfully processed for up to eight passes using this method. Quantitative microstructural analysis revealed a remarkable grain refinement, with the average grain size reduced from an initial 77.76 µm to 21.28 µm and 10.72 µm after four and eight passes, respectively, corresponding to an 86% total reduction. This refinement produced a microstructure ideally suited for superplastic forming, dominated by high-angle grain boundaries. Subsequent uniaxial tensile tests demonstrated exceptional superplasticity, with maximum elongations to failure of 340% and 580% achieved at 683 K and a strain rate of 2×10^{-4} s^{-1} for the four-pass and eight-pass samples, respectively. The eight-pass sample also exhibited a lower flow stress, confirming a transition of the dominant deformation mechanism to grain boundary sliding. The ECAP-Pull process represents a significant advancement by overcoming the batch-processing bottleneck of traditional SPD methods, offering a scalable and industrially viable route for producing superplastic sheet materials.

1. Introduction

Improving the physical and mechanical properties of alloy components is essential for ensuring reliable performance under anticipated loading and temperature conditions, as well as for reducing secondary costs. In this regard, refinement of the average grain size through severe plastic deformation (SPD) techniques has emerged as one of the most effective strategies for enhancing the strength of metallic alloys, as described by the Hall–Petch relationship:

$$\sigma_y = \sigma_0 + k_y d^{-1/2} \quad (1)$$

where σ_y represents the yield stress, σ_0 is the friction stress, k_y is the material's yield constant, and d denotes the average grain size. Beyond improving strength, grain refinement via SPD also promotes the formation of fine,

* Corresponding author
E-mail address: m.keshtiban@mee.uut.ac.ir (P. Mashhadi Keshtiban)
https://doi.org/10.22099/IJMF.2026.54698.1358

equiaxed microstructures, which facilitate grain boundary sliding during high-temperature deformation, thereby significantly enhancing the alloy's formability.

Valiev [1] reported remarkable improvements in the physical and mechanical properties of various metals and alloys subjected to SPD, including enhanced superplasticity, mechanical strength, formability, and fatigue resistance. Horita et al. [2] refined the grain size of a magnesium-based alloy to approximately 1 μm through a two-step process involving direct extrusion (extrusion ratio of 1:36) followed by hot ECAP, achieving a fourfold increase in elongation during uniaxial tensile testing. Yang et al. [3] examined the superplastic behavior of the LA91 magnesium alloy under a two-step uniaxial tensile testing procedure. Their results demonstrated that an initial tensile stage with a constant strain rate, followed by a tensile stage involving strain rate sensitivity optimization, significantly improveed the alloy's plastic deformation capability, thereby facilitating the fabrication of components with complex geometries. Azizi and Mahmoudi [4] observed considerable grain refinement and expansion of dynamically recrystallized regions in Mg-xGd alloys after six-pass multidirectional forging, confirming the process's potential for superplasticity with a strain-rate sensitivity (m) of 0.48.

Yang et al. [5] examined the effect of strain-rate sensitivity and temperature on Mg–9Li–1Al alloys, finding that maximum elongation was achieved after eight ECAP passes at peak sensitivity, while exceeding the permissible processing temperature led to oxidation and unstable microstructures. Sergueeva et al. [6] reported significant pre-fracture elongation in Ti-6Al-4V alloys refined via high-pressure torsion (HPT), highlighting HPT's suitability for low-volume production of high-performance parts. Alizadeh et al. [7] compared HPT, ECAP, and extrusion in Mg-Gd-Y-Zr alloys and identified HPT as the most effective method for enhancing superplasticity due to superior grain refinement, energy efficiency, and high tensile elongation with minimal fracture. Xu et al. [8] determined optimal ECAP passes for 2024 and 7034 aluminum alloys to achieve the best superplastic behavior during uniaxial tensile testing.

Further studies demonstrated the influence of high-pressure and temperature-assisted processes on superplasticity in various alloys. Takizawa et al. [9] achieved 400% elongation in Inconel 718 using high-pressure sliding at room temperature, while Islamgaliev et al. [10] emphasized that, besides grain refinement, the presence of precipitates, high-angle grain boundaries, and precise temperature control are essential prerequisites in achieving superplasticity in 1420 and 1421 aluminum alloys. Kawasaki and Langdon [11] reported that the highest elongation of Zn-22%Al alloy strips occurred at a strain rate of 1×10^{-2} s^{-1} after eight ECAP passes, with grain boundary sliding as the controlling deformation mechanism. Musin et al. [12] observed two distinct fracture mechanisms in an Al-Mg-Sc alloy: ductile necking at low temperatures/high strain rates, and brittle fracture without necking at elevated temperatures/low strain rates.

Post-ECAP rolling was found to further enhance superplasticity. Park et al. [13] demonstrated that a combination of four ECAP passes with a 70% thickness reduction in aluminum 5154 achieved a similar high-strain-rate superplasticity as eight ECAP passes alone. Nikulin et al. [14] showed that isothermal rolling at 250 °C after ECAP increased the number of high-angle grain boundaries in aluminum 7055, improving its plastic properties. Islamgaliev et al. [15] reported that optimal grain refinement (0.3–0.4 μm) in aluminum 1421 was achieved at 370 °C, yielding a maximum elongation of 1500% during uniaxial tensile testing at 400 °C. Turba et al. [16] observed submicron particle formation and high strain-rate sensitivity ($m > 0.6$) in an Al-Mg-Zr-Sc alloy after ECAP, attributed to the stability of $Al_3(Zr_xSc_{1-x})$ precipitates.

Several studies focused on aluminum-magnesium-scandium alloys. Komura et al. [17] optimized ECAP processing of Al-3%Mg-0.2%Sc alloys, achieving true strains of at least 8 after eight passes, which led to improved formability and homogeneous high-angle grain boundaries. Miyahara et al. [18] reported that extrusion at 623 K (ratio 1:36) followed by two-stage ECAP at 473 K and subsequent annealing ensured

microstructural stability in Zr-containing Mg-7.5%Al-0.2%Zr alloys. Matsubara et al. [19] investigated the microstructural refinement of the Mg-9%Al alloy using a combined extrusion and equal channel angular pressing (EX-ECAP) process. Their analysis indicated that due to the occurrence of concurrent grain growth and excessive grain boundary sliding during the process, it is recommended that the ECAP procedure be performed at a temperature below 573 K for this specific alloy. Figueiredo and Langdon [20] identified an optimal strain rate of 2×10^{-4} s^{-1} for superplasticity in the ZK60 magnesium alloy, with deviations reducing elongation. Higashi [21] highlighted the role of grain refinement, microstructural stability, and soft or amorphous phases in mitigating stress concentrations at high strain rates. Mikhaylovskaya et al. [22] confirmed that superplastic deformation in an Al-(3.5-4.5)Zn-(3.5-4.5)Mg-(0.7-0.9)Cu-(1.0-3.0)Ni-(0.25-0.30)Zr alloy with an average grain size of 1.8 µm, can be achieved at 380-480 °C and strain rates of 0.002-0.1 s^{-1}.

Perevezentsev et al. [23] achieved superplasticity in the 1570 aluminum alloy via five HPT passes at 400 °C, while Sakai et al. [24] processed disk-shaped samples of the Al-3%Mg-0.2% Sc alloy through five passes of HPT under a pressure of 6 GPa. The results of hot tensile testing indicated that the material achieved ultimate strength and elongation comparable to that obtained by the ECAP process at 673 K and a strain rate of 3.3×10^{-2} s^{-1}. Kim et al. [25] determined that eight to twelve 90° ECAP passes optimized superplasticity in 6061 aluminum. Avtokratova et al. [26] obtained ultra-high elongation (4100%) in an Al-5Mg-0.18Mn-0.2Sc-0.08Zr-0.01Fe-0.01Si alloy at 450 °C and a strain rate of 0.056 s^{-1} with an average grain size of 1 µm. Bobruk et al. [27] achieved 240% elongation with a strain-rate sensitivity of 0.31 in 6061 aluminum strips processed via ECAP at 160–250 °C. Mogucheva et al. [28] reported 1440% elongation in 5024 aluminum using ECAP and cold rolling at 400–450 °C with strain rates of 0.014–0.56 s^{-1}. Soliman and Abo-Elkhier [29] studied the superplastic behavior of the 7475 aluminum alloy with an average grain size of 10 µm, obtained through thermomechanical processing, using high-temperature tensile testing. They observed that increasing strain rate enhanced strain-hardening in 7475 aluminum at constant temperature, whereas increasing temperature at a constant strain rate reduced flow stress.

However, the widespread industrial adoption of these SPD techniques is constrained by significant scalability challenges. Methods like high-pressure torsion (HPT) are inherently limited to small, discrete samples [6, 7], while the more versatile equal channel angular pressing remains a batch process. The requirement to process individual billets in ECAP leads to low production rates, high energy consumption per unit volume, and difficulties in achieving microstructural homogeneity over long lengths, preventing its seamless integration into continuous manufacturing lines. This highlights a critical gap for a deformation strategy that retains the fundamental grain-refining shear mechanics of SPD while enabling a more practical, scalable processing route for industrial-scale components. To address these scalability limitations, the ECAP-Pull technique has been developed. This method replaces the pressing action with a pulling mechanism, which is particularly suited for processing sheet or strip material in a more continuous fashion, thereby overcoming the batch-processing bottleneck of conventional ECAP. Moreover, given the limited studies on the superplastic behavior of aluminum 1050, the present work investigates the superplastic properties of this alloy processed via the proposed SPD method.

2. Materials and Method

In the proposed SPD method, unlike the conventional ECAP process [30, 31], the sample is subjected to tensile rather than compressive loading to apply force and guide it through the die. In other words, the aforementioned process has been modified into the ECAP-Pull method. This modification simplifies the procedure, eliminates certain common issues encountered in traditional ECAP processes enhances efficiency in specific cases, increases the service life of the die, and-most importantly-reduces the required power consumption and energy losses during the process.

2.1. Material preparation

In the present study, strips of commercial aluminum alloy AA1050, with a high purity of 99.5% and dimensions of 1 mm × 20 mm × 1100 mm, were used as test specimens. The results of the quantitative chemical composition analysis and the mechanical properties of the selected alloy are presented in Tables 1 and 2, respectively.

Several important factors were considered in selecting the sample dimensions:

• The width of the processed specimen (regardless of its composition) must be less than 20 mm with appropriate tolerances, corresponding to the width of the fabricated die channel.

• Determining the sample thickness is crucial, as it depends directly on the die channel thickness and angles, the tensile strength of the strip, the maximum load-bearing capacity of the die, and the power capability of the tensile system used.

• The sample length must be chosen according to the maximum stroke length of the process.

2.2. Die design

Fig. 1(a) illustrates the schematic drawing of the designed die. As shown, the die consists of three channels intersecting at an angle of 90°, through which the aluminum strip is drawn through. Fig. 1(b) shows the two halves of the die. Initially, the alloy strip must be bent according to the shape of the die channel and then positioned inside the channel. Subsequently, other half of the die was placed, and the die was firmly fastened using seventeen semi-threaded bolts. The primary function of these bolts is to withstand the load applied to the billets from the lateral surfaces of the metal strip.

The schematic of the alloy grain refinement process is shown in Fig. 1(c). After the complete assembly of the die, it is secured to a rigid support (the blue component) using a simple pin. Simultaneously, the alloy strip is pulled through the die by a tensile force applied from the side opposite to the locking pin.

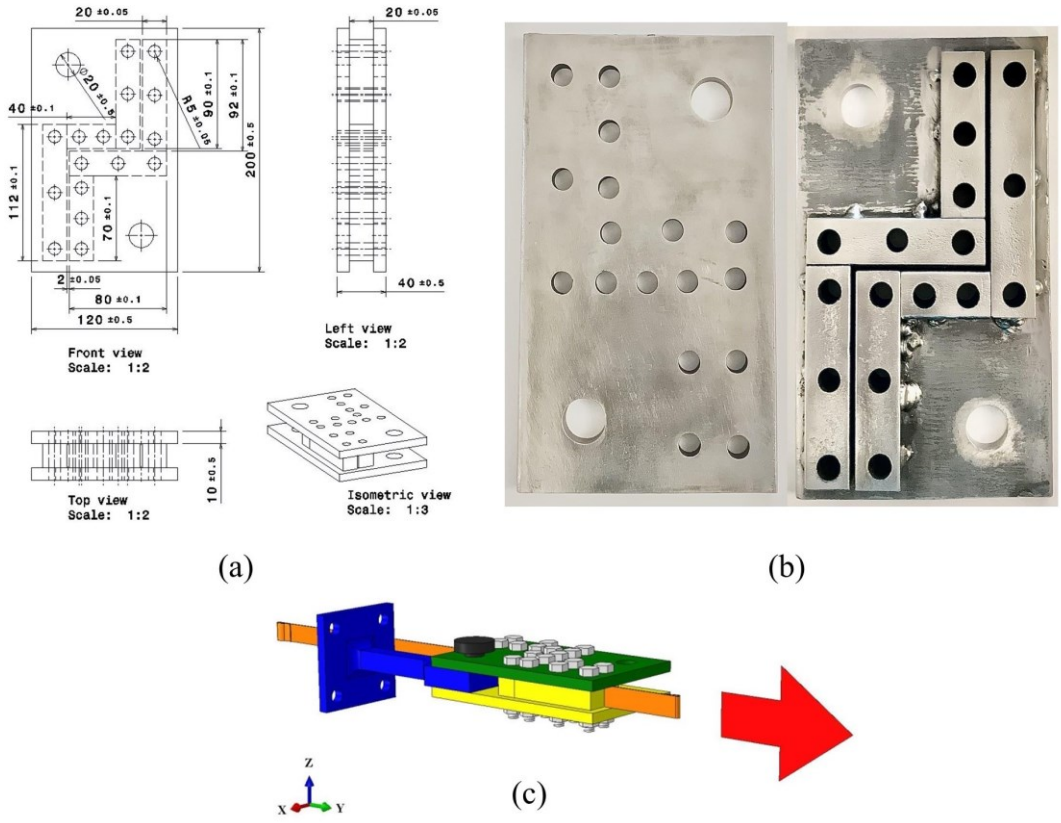

Fig. 1. (a) Drawing of the die, (b) lower and upper halves of the manufactured die, and (c) schematic of the process.

Table 1. Chemical composition of aluminum alloy 1050 (wt.%)

Si	Fe	Cu	Mn	Mg	Zn	Ti
0.10154	0.25277	0.00672	0.04187	0.01537	0.02269	0.04327
Cr	**Ni**	**Pb**	**Sn**	**V**	**Sb**	**Al**
0.00120	0.00406	0.00828	0.00001	0.01198	0.00967	99.4999

Table 2. Mechanical properties of aluminum alloy 1050 [32]

Parameter	Value
Young's modulus (E)	69 GPa
Poisson's ratio (ν)	0.33
Density (ρ)	2700 kg/m^3
Thickness (t)	1 mm

It is crucial that the applied force on the metallic strip be aligned with the line passing through the central axis of the die's outlet channel and the center of the locking pin. It should be noted that when multiple processing passes are required, the strip should not be completely withdrawn from the die; a few centimeters of the strip must remain outside on the inlet side.

For additional processing passes, it is necessary to release the die from both the pulling device and the locking pin, rotate the die 180° about the vertical axis, secure it again by the pin on the previously used outlet side, and pull the strip outward from the remaining excess length produced in the previous pass.

In the present study, alloy strips with dimensions of 20 mm × 1100 mm were processed using this method- one strip through four passes and another through eight passes. It should be emphasized that, unlike the conventional single-pass ECAP process [33, 34], this method does not require the material to be processed through different routes to achieve a homogeneous structure across the specimen's cross-section, since in each pass, both lateral surfaces of the strip remain in contact with the die channel corners.

This methodology confers several distinct advantages. Primarily, it eliminates the need for sample reorientation between successive processing passes, as each corner of the die maintains in continuous contact with a lateral surface of the strip. Furthermore, the process obviates the use of a punch, thereby circumventing the challenges associated with its fabrication and implementation. The absence of hydrostatic pressure within the die channel leads to a reduction in the power required for processing. Additionally, die wear is minimized due to reduced energy consumption and the optimal direction of the applied force. This not only extends the service life of the die but also permits its construction from less wear-resistant materials, yielding significant cost savings in raw materials and manufacturing. The technique also eliminates the necessity for precise alignment between the sample's longitudinal axis and the die channel or the applied force. A notable increase in the speed of the ECAP process is achieved by transforming it into a continuous SPD (CSPD) operation, which can be performed without specialized high-pressure equipment. There are no constraints on the length of the sample, allowing for the processing of extensive strips. The significant reduction in the wear area and friction at the sample-die interface considerably enhances die longevity and reduces parasitic power loss.

2.3. Superplastic behavior

After completing the microstructural refinement process, dog-bone tensile specimens were machined from the central region of the strips processed through four- and eight-pass conditions. Tensile specimens were prepared according to Fig. 2, with a gauge length of 10 mm, aligned parallel to the processing direction. Sample fabrication was carried out using wire electrical discharge machining (EDM).

Based on the optimized test conditions reported in previous studies on the superplastic behavior of commercial 1050 aluminum alloy [35], each billet of

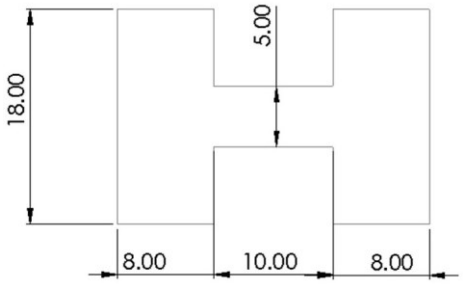

Fig. 2. Dog-bone specimens' dimensions (mm).

dog-bone specimens, processed through four or eight passes via the proposed method, was evaluated using a uniaxial hot tensile testing machine. To investigate the superplastic behavior tests were conducted at temperatures of 663 °C and 683 °C with constant true strain rates of 2×10^{-4} s^{-1} and 2×10^{-3} s^{-1} [36]. In order to ensure uniform temperature distribution throughout the gauge section, each specimen was held in a preheated furnace for 10 minutes prior to the start of the tensile tests.

2.4. Microstructural characterization

After processing, the samples underwent a sequence of metallographic preparation steps. First, a small hole was drilled into each sample to accommodate a copper wire for electrical connection during subsequent electrochemical steps. Both ends of the hole were then soldered to seal the interface; this critical step prevents polyester mounting resin from infiltrating the hole and disrupting the electrical contact. Following this, the samples were mounted in polyester resin.

The mounted samples were then mechanically ground using progressively finer silicon carbide sandpaper, starting from 100 grit and proceeding to 2500 grit. The grinding direction was rotated 90° between each grit change to ensure uniform material removal and to eliminate scratches from the previous stage.

Next, the samples were electropolished to achieve a smooth, deformation-free surface and to suitable them for etching. Electropolishing utilized the electrolyte specified in Table 3. A DC power supply was set to 25 V, with the sample as the anode and a 304 stainless steel plate as the cathode. The process duration was 20 seconds. After electropolishing, the samples were rinsed with ethanol and dried thoroughly.

Subsequently, electrochemical etching was conducted to reveal the grain structure. The setup was identical to that used for electropolishing (25 V, 304 stainless steel cathode), but a different electrolyte (Table 4) and a longer duration of 3 minutes were employed. Throughout both electrochemical steps, care was taken to maintain precise parallel alignment between the sample (anode) and the cathode. After etching, the samples were again rinsed with ethanol and dried.

Finally, the microstructures were examined using an optical microscope (Olympus PMG3). The grain size distribution was quantitatively analyzed according to the ASTM E112 standard. This was achieved by applying the linear intercept method to the micrographs using ImageJ software to determine the average grain size after each stage of processing [37].

Table 3. Composition of the electrolyte solution in the electro-polish step

Ethanol	$HClO_4$	
40	160	Required amount (ml)

Table 4. Composition of the electrolyte solution in electro-chemical etching step

Deionized water	HBF4	
2	100	Required amount (ml)

3. Results and Discussion

3.1. Grain refinement

For the initial alloy strips (Fig. 3(a)), the largest measured grain size was 320.08 µm, with an average grain size of 77.76 µm. Approximately 21% of the observed grains in the image were smaller than 25 µm. The grain density was calculated to be 210.677 [1/mm²]. The initial coarse grain size of the 1050 aluminum alloy is primarily attributed to the prior cold rolling and the partial thickness reduction to obtain a 1 mm sheet.

After four passes (Fig. 3(b)), the average grain size in the processed strip decreased to 21.28 µm, representing a 72.63% reduction compared to the initial specimen. The largest observed grain measured 205.78 µm, and the grain density in the unit area reached 2813.112 [1/mm²]. Notably, 71% of the grains after four passes had sizes below 25 µm.

After processing, the metallographic images of the eight-pass processed 1050 aluminum specimens (Fig. 3(c)) show that approximately 98% of the grains are smaller than 25 µm. The maximum recorded grain size is 95.14 µm, and the average size of the ultrafine grains is measured at 10.72 µm, corresponding to an 86.21% reduction compared to the initial sample. The grain density in the unit area is 11085.13 [1/mm²]. The reported

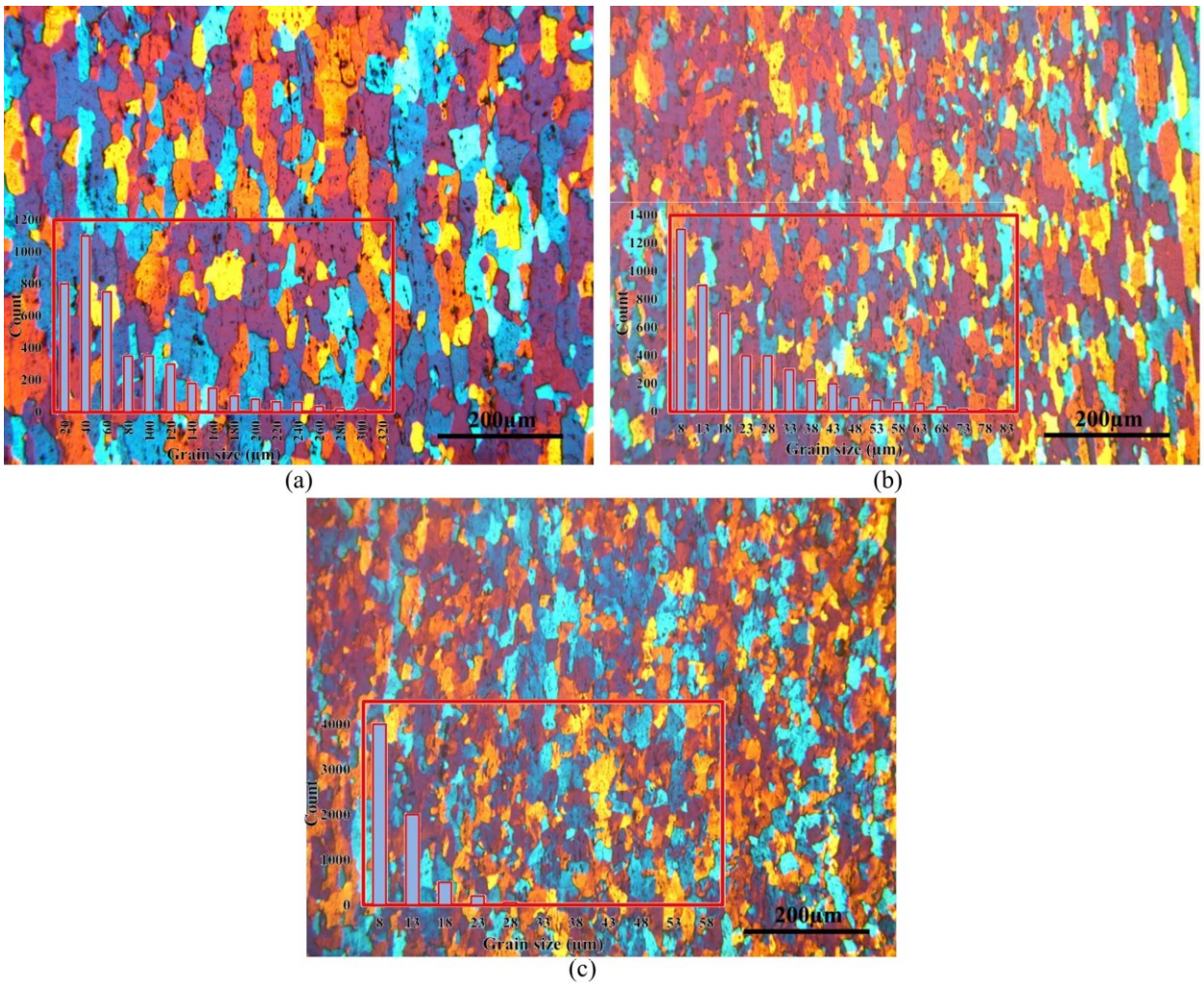

Fig. 3. Metallographic images and statistical processing obtained for (a) the initial specimens, (b) four-pass and (c) eight-pass processed strips.

average grain sizes now include the standard deviation for initial: 77.76 ± 100.83 μm, 21.28 ± 29.77 μm, 10.72 ± 11.12 μm.

An important observation, based on Figs. 3(c) and 3(b) as well as statistical processing charts, is that increasing the number of processing passes does not significantly affect the further refinement of the smallest grains. However, the number of coarse grains decreases noticeably after each pass, and their refinement tends to align more homogeneously along the processing direction (Table 5).

3.2. Analysis of the superplastic behavior of processed samples

Fig. 4 presents the deformed specimens of commercial aluminum alloy 1050 after superplastic deformation tests, together with the corresponding experimental parameters and measured elongations. The results demonstrate that the maximum elongation to failure reached approximately 580% and 340% for the eight-pass (Fig. 4(b)) and four-pass (Fig. 4(a)) processed samples, respectively, when tested at a strain rate of 2×10^{-4} s^{-1} and a temperature of 683 K.

In contrast, the four-pass processed sample tested at a higher strain rate of 1×10^{-3} s^{-1} and a temperature of 663 K exhibited an elongation of only 190%, which falls below the generally accepted threshold of 200% required to confirm superplasticity under uniaxial tensile conditions.

As observed in Fig. 4, deformation occurred uniformly along the entire gauge length, resulting in a fully homogeneous elongation without the appearance of localized necking. Such uniform deformation behavior is indicative of a stable superplastic flow regime. To

Table 5. Grain size distribution

	Count	Min (μm)	Max (μm)	Average (μm)	Std
Initial	4369	0.89	320.08	77.76	100.83
4-pass	4809	0.89	205.78	21.28	26.77
8-pass	6815	0.89	95.14	10.72	11.12

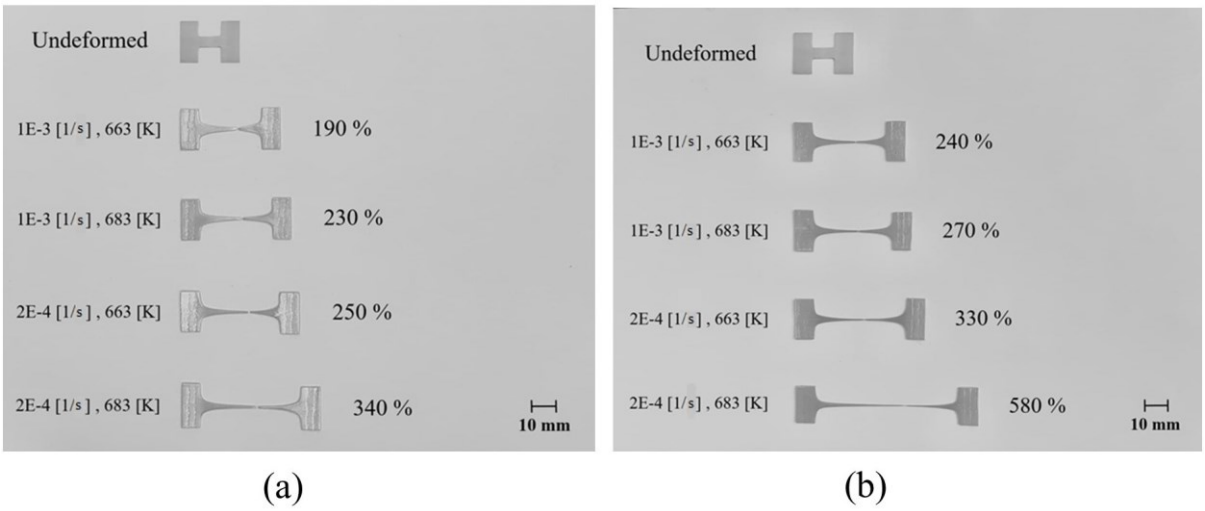

Fig. 4. Hot tensile tests results of samples after (a) four-passes and (b) eight-passes of processing.

achieve large tensile strains in uniaxial testing, the presence of an equiaxed microstructure with a high fraction of high-angle grain boundaries (HAGBs, $\theta > 16°$) is essential. These boundaries play a critical role in promoting superplasticity, as material flow during this process is predominantly governed by the grain boundary sliding (GBS) mechanism.

Stress–strain curves obtained from the uniaxial tensile tests of the commercial aluminum alloy 1050 are presented in Fig. 5. As can be seen, due to the occurrence of strain softening within the deformation region under critical temperature conditions, the peak flow stress prior to fracture decreases with an increasing number of processing passes. Moreover, a reduction in temperature and an increase in strain rate during tensile testing lead to an enhancement in the maximum flow stress.

The reduction in peak flow stress and the significant enhancement in elongation after eight passes, as shown in Figs. 4 and 5, can be attributed to the more refined and stable ultrafine-grained microstructure (Fig. 3(c)). The higher number of passes leads to a greater accumulation of high-angle grain boundaries (HAGBs). A higher fraction of HAGBs is crucial for enabling grain boundary sliding (GBS), which is the primary mechanism of superplastic deformation. Consequently, the eight-pass sample accommodates strain more efficiently through GBS at a lower flow stress, resulting in superior ductility. In contrast, the four-pass sample, with a coarser microstructure and fewer HAGBs, exhibits a higher resistance to deformation (higher flow stress) and a reduced capacity for GBS, leading to lower elongation.

Based on the range of experimental variables examined, the optimum parameters for achieving the maximum uniaxial superplastic elongation in aluminum alloy 1050 can be identified as a temperature of 683 K, a strain rate of 2×10^{-4} s^{-1}, and microstructural refinement achieved through eight processing passes.

The superplastic behavior of the processed AA1050 alloy exhibits a strong dependence on both strain rate and temperature, which is characteristic of a deformation mechanism controlled by grain boundary sliding (GBS). The significant increase in elongation from 190% (at 1×10^{-3} s^{-1}) to 340% and 580% (at 2×10^{-4} s^{-1}) for the four-pass and eight-pass samples, respectively, can be rationalized by the strain rate sensitivity index (m-value). A higher m-value indicates a greater resistance to

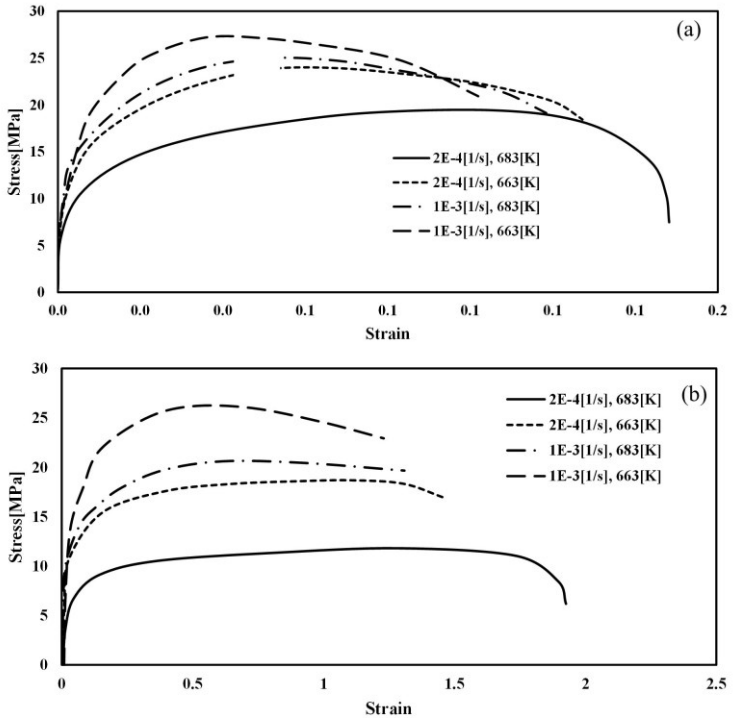

Fig. 5. Stress–strain curves: (a) four-pass and (b) eight-pass processed samples.

necking and is a fingerprint of superplasticity. The lower strain rate (2×10^{-4} s^{-1}) allows sufficient time for diffusional processes (accommodation mechanisms) to operate at grain boundaries, facilitating sustained GBS without premature void formation or fracture. Conversely, at the higher strain rate ($1\times10^{-}3$ s^{-1}), these accommodation processes cannot keep pace with the imposed deformation, leading to stress concentrations, limited GBS, and consequently, lower ductility.

A detailed strain rate sensitivity analysis was performed. The m-values were determined from the slopes of linear regressions fitted to ln (σ) vs. ln (ė) plots for each processing condition (four and eight passes) at the two testing temperatures.

As shown in the newly added Fig. 6, the m-values exhibit a clear dependence on both the number of passes and the temperature. For the eight-pass samples, the m-values are 0.35 at 683 K and 0.21 at 663 K, confirming that the material enters the superplastic regime ($m > 0.3$) at the higher temperature after sufficient grain refinement. For the four-pass samples, the corresponding m-values drop to 0.16 at 683 K and 0.08 at 663 K, indicating that the microstructure after four passes is still predominantly deformed by dislocation-based mechanisms,

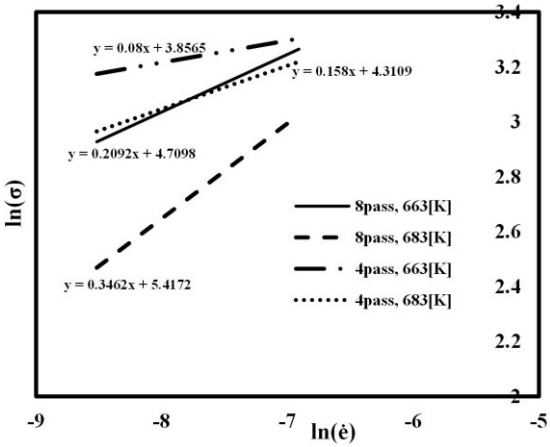

Fig. 6. ln (σ) vs. ln (ė) plots for different passes and temperatures.

with only limited contribution from grain-boundary sliding.

These results quantitatively support our earlier observations. The superior superplastic elongation (≈580 %) of the eight-pass sample at 683 K is directly linked to its higher strain-rate sensitivity ($m \approx 0.35$), which suppresses necking and promotes homogeneous deformation.

4. Conclusions

In the present work, based on the fundamental principles

and previous studies, the necessity of developing practical solutions to facilitate processing, reduce energy consumption, and improve efficiency in one of the most conventional and long-established SPD techniques, namely ECAP, was identified. Accordingly, an innovative approach was introduced that involves fundamental modifications to the die design and operational mechanism, aimed at enhancing the overall performance of the process. Ultimately, the superplastic behavior of aluminum alloy 1050 strips processed by the newly proposed ECAP-Pull method was analyzed from both metallurgical and mechanical perspectives.

The main findings can be summarized as follows:

The average grain size of the 1 mm-thick aluminum 1050 alloy strip was reduced by 70.26% and 86.26%, achieving mean grain sizes of 21.28 μm and 10.72 μm after four and eight passes, respectively.

The ECAP process was simplified through the reduction of die geometric parameters, the elimination of the plunger, and the removal of route-changing steps in consecutive passes. Furthermore, the process no longer requires high-pressure loading equipment, nor the use of complex or high-strength materials for die fabrication.

The processing speed was improved by transforming the conventional SPD method into a continuous SPD system, enabling the processing of long aluminum strips within a short period of time.

The proposed method offers the capability to extend applicability to materials with different mechanical properties and thicknesses by designing adaptive dies with adjustable channel angles.

The maximum elongations of 580% and 340% were obtained during uniaxial tensile testing of the processed aluminum alloy 1050 at a constant strain rate of 2×10^{-4} s^{-1} and a temperature of 683 K, corresponding to the samples processed through eight and four passes, respectively.

The formability and ductility of the alloy at elevated temperatures were significantly improved owing to uniform grain refinement and the formation of high-angle grain boundaries (HAGBs) induced by the process, which facilitated grain boundary sliding and consequently enhanced superplastic deformation.

Authors' contributions

A. Taher: Writing original draft, Data collection, Date analysis

P. Mashhadi Keshtiban: Supervision, Writing - review & editing

Conflict of interest

The authors declare that they have no financial or personal relationships that could have inappropriately influenced or biased the work presented in this manuscript.

Funding

This research received no external funding.

5. References

[1] Valiev, R. (2001). Developing SPD methods for processing bulk nanostructured materials with enhanced properties. *Metals and Materials International*, *7*(5), 413-420. https://doi.org/10.1007/BF03027081

[2] Horita, Z., Matsubara K., Makii K., & Langdon T. G. (2002). A two-step processing route for achieving a superplastic forming capability in dilute magnesium alloys. *Scripta Materialia*, *47*(4), 255-260. https://doi.org/10.1016/S1359-6462(02)00135-5

[3] Yang, H., Zhang, X., Chen, P., Fu, M., Wang, G., & To, S. (2019). Investigation on the enhanced maximum strain rate sensitivity (m) superplasticity of Mg-9Li-1Al alloy by a two-step deformation method. *Materials Science and Engineering: A, 764*, 138219. https://doi.org/10.1016/j.msea.2019.138219

[4] Azizi, N., & Mahmudi, R. (2019). Superplasticity of fine-grained Mg–xGd alloys processed by multi-directional forging. *Materials Science and Engineering A*, *767*, 138436. https://doi.org/10.1016/j.msea.2019.138436

[5] Yang, H., Fu, M., To, S., & Wang, G. (2016). Investigation on the maximum strain rate sensitivity (m) superplastic deformation of Mg-Li based alloy. *Materials & Design*, *112*, 151-159. https://doi.org/10.1016/j.matdes.2016.09.066

[6] Sergueeva, A., Stolyarov, V., Valiev, R., & Mukherjee, A. (2000). Enhanced superplasticity in a Ti-6Al-4V alloy processed by severe plastic deformation. *Scripta Materialia*, *43*(9), 819-824. https://doi.org/ 10.1016/S1359-6462(00)00496-6

[7] Alizadeh, R., Mahmudi, R., Pereira, P., Huang, Y., & Langdon, T. (2017). Microstructural evolution and superplasticity in an Mg–Gd–Y–Zr alloy after processing by different SPD techniques. *Materials Science and*

Engineering A, *682,* 577-585. https://doi.org/10.1016/j.msea.2016.11.080

[8] Xu, C., Furukawa, M., Horita, Z., & Langdon, T. G. (2003). Achieving a superplastic forming capability through severe plastic deformation. *Advanced Engineering Materials*, *5*(5), 359-364. https://doi.org/10.1002/adem.200310075

[9] Takizawa, Y., Kajita, T., Kral, P., Masuda, T., Watanabe, K., Yumoto, M., Otagiri, Y., Sklenicka, V., & Horita, Z. (2017). Superplasticity of Inconel 718 after processing by high-pressure sliding (HPS). *Materials Science and Engineering A*, *682,* 603-612. https://doi.org/10.1016/j.msea.2016.11.081

[10] Islamgaliev, R. K., Yunusova, N. F., & Valiev, R. (2006, January). The influence of the SPD temperature on superplasticity of aluminium alloys. In *Materials Science Forum* (Vol. 503, pp. 585-590). Trans Tech Publications Ltd. https://doi.org/10.4028/www.scientific.net/MSF.503-504.585

[11] Kawasaki, M., & Langdon, T. G. (2009). Flow behavior of a superplastic Zn–22% Al alloy processed by equal-channel angular pressing. *Materials Science and Engineering A*, *503* (1-2), 48-51. https://doi.org/10.1016/j.msea.2008.04.081

[12] Musin, F., Kaibyshev, R., Motohashi, Y., & Itoh, G. (2004). Superplastic behavior and microstructure evolution in a commercial Al-Mg-Sc alloy subjected to intense plastic straining. *Metallurgical and Materials Transactions A*, *35*(8), 2383-2392. https://doi.org/10.1007/s11661-006-0218-4

[13] Park, K. T., Lee, H. J., Lee, C. S., Nam, W. J., & Shin, D. H. (2004). Enhancement of high strain rate superplastic elongation of a modified 5154 Al by subsequent rolling after equal channel angular pressing. *Scripta Materialia*, *51*(6), 479-483. https://doi.org/10.1016/J.SCRIPTAMAT.2004.06.001

[14] Nikulin, I., Kaibyshev, R., & Sakai, T. (2005). Superplasticity in a 7055 aluminum alloy processed by ECAE and subsequent isothermal rolling. *Materials Science and Engineering: A*, *407*(1-2), 62-70. https://doi.org/10.1016/j.msea.2005.06.014

[15] Islamgaliev, R., Yunusova, N., Valiev, R., Tsenev, N., Perevezentsev, V., & Langdon, T. (2003). Characteristics of superplasticity in an ultrafine-grained aluminum alloy processed by ECA pressing. *Scripta Materialia*, *49*(5), 467-472. https://doi.org/10.1016/S1359-6462(03)00291-4

[16] Turba, K., Málek, P., & Cieslar, M. (2007). Superplasticity in an Al–Mg–Zr–Sc alloy produced by equal-channel angular pressing. *Materials Science and Engineering: A*, *462*(1-2), 91-94. https://doi.org/10.1016/j.msea.2006.01.178

[17] Komura, S., Furukawa, M., Horita, Z., Nemoto, M., & Langdon, T. G. (2001). Optimizing the procedure of equal-channel angular pressing for maximum superplasticity. *Materials Science and Engineering: A*, *297*(1-2), 111-118. https://doi.org/10.1016/S0921-5093(00)01255-7

[18] Miyahara, Y., Matsubara, K., Horita, Z., & Langdon T. G. (2005). Grain refinement and superplasticity in a magnesium alloy processed by equal-channel angular pressing. *Metallurgical and Materials Transactions A*, *36*(7), 1705-1711. https://doi.org/10.1007/s11661-005-0034-2

[19] Matsubara, K., Miyahara, Y., Horita, Z., & Langdon, T. (2003). Developing superplasticity in a magnesium alloy through a combination of extrusion and ECAP. *Acta Materialia*, *51*(11), 3073-3084. https://doi.org/10.1016/S1359-6454(03)00118-6

[20] Figueiredo, R. B., & Langdon, T. G. (2006). The development of superplastic ductilities and microstructural homogeneity in a magnesium ZK60 alloy processed by ECAP. *Materials Science and Engineering: A*, *430*(1-2), 151-156. https://doi.org/10.1016/j.msea.2006.05.056

[21] Higashi, K. (1994, October). Deformation mechanisms of positive exponent superplasticity in advanced aluminum alloys with nano or near-nano scale grained structures. In *Materials Science Forum* (Vol. 170, pp. 131-140). Trans Tech Publications Ltd. https://doi.org/10.4028/www.scientific.net/MSF.170-172.131

[22] Mikhaylovskaya, A., Kotov, A., Pozdniakov, A., & Portnoy, V. (2014). A high-strength aluminium-based alloy with advanced superplasticity. *Journal of Alloys and Compounds*, *599*, 139-144. https://doi.org/10.1016/j.jallcom.2014.02.061

[23] Perevezentsev, V., Shcherban, M. Y., Murashkin, M. Y., & Valiev, R. (2007). High-strain-rate superplasticity of nanocrystalline aluminum alloy 1570. *Technical Physics Letters*, *33*(8), 648-650. https://doi.org/10.1134/S106378500708007X

[24] Sakai, G., Horita, Z., & Langdon, T. G. (2005). Grain refinement and superplasticity in an aluminum alloy processed by high-pressure torsion. *Materials Science and Engineering: A*, *393*(1-2), 344-351. https://doi.org/10.1016/j.msea.2004.11.007

[25] Kim, W., Kim, J., Park, T., Hong, S., Kim, D., Kim, Y., & Lee, J. (2002). Enhancement of strength and superplasticity in a 6061 Al alloy processed by equal-channel-angular-pressing. *Metallurgical and Materials Transactions A*, *33*(10), 3155-3164. https://doi.org/10.1007/s11661-002-0301-4

[26] Avtokratova, E., Sitdikov, O., Markushev, M., & Mulyukov, R. (2012). Extraordinary high-strain rate

superplasticity of severely deformed Al–Mg–Sc–Zr alloy. *Materials Science and Engineering: A*, *538*, 386-390. https://doi.org/10.1016/j.msea.2012.01.041

[27] Bobruk, E. V., Safargalina, Z. A., Golubev, O. V., Baykov, D., & Kazykhanov, V. U. (2019). The effect of ultrafine-grained states on superplastic behavior of Al-Mg-Si alloy. *Materials Letters*, *255*, 126503. https://doi.org/10.1016/j.matlet.2019.126503

[28] Mogucheva, A., Yuzbekova, D., & Kaibyshev, R. (2016, February). Superplasticity in a 5024 aluminium alloy subjected to ECAP and subsequent cold rolling. In *Materials Science Forum* (Vol. 838, pp. 428-433). Trans Tech Publications Ltd. https://doi.org/10.4028/www.scientific.net/MSF.838-839.428

[29] Abo-Elkhier, M., & Soliman, M. S. (2006). Superplastic characteristics of fine-grained 7475 aluminum alloy. *Journal of Materials Engineering and Performance*, *15*(1), 76-80. https://doi.org/10.1361/105994906X83394

[30] Keshtiban, P. (2020). Microstructural evolutions during the ecmap process using the die with optimum geometrical parameters. *Metallography, Microstructure, and Analysis*, *9*(4), 596-602. https://doi.org/10.1007/s13632-020-00664-z

[31] Keshtiban, .P, Behnagh, R. A., Bashirzadeh, F., Javadzadeh, R., & Mohsenzadeh, A. (2021). Investigation on the anisotropy behavior of copper strips processed by a combination of FSP and ECAP. *Proceedings of the Institution of Mechanical Engineers, Part L: Journal of Materials: Design and Applications, 235*(8), 1890-1900. https://doi.org/10.1177/146442072110095

[32] Keshtiban, P., Zadshakouyan, M., & Faraji, G. (2015). Modeling and production of high strength Al strips by equal channel multi angular pressing method. *Journal of Advanced Materials and Processing*, *3*(4), 3-10.

[33] Keshtiban, P., & Bashirzadeh, F. (2017). Die and process parameters effects on ECAP process of sheet-type samples. *Metallography, Microstructure, and Analysis*, *6*(6), 463-469. https://doi.org/10.1007/s13632-017-0389-y

[34] Kestiban, P., Behnagh, R., & Alimirzaloo, V. (2018). Routes ivestigation in equal channel multi-angular pressing process of UFG Al− 3% Mg alloy strips. *Transactions of the Indian Institute of Metals*, *71*(3), 659-664. https://doi.org/10.1007/s12666-017-1198-3

[35] Nagy M., Abd El-Salam, F., Habib, N., & Kamel, R. (1981).Grain boundary sliding as the origin of superplasticity in commercially pure aluminium. *Materials Science and Engineering, 47*(1), 23-28. https://doi.org/10.1016/0025-5416(81)90036-7

[36] Mishra R. S., Valiev, R., McFadden, S., Islamgaliev, R., & Mukerjee, A. (2001). High-strain-rate superplasticity from nanocrystalline Al alloy 1420 at low temperatures. *Philosophical Magazine A*, *81*(1), 37-48. https://doi.org/10.1080/01418610108216616

[37] Keshtiban, P., & Bashirzadeh, F. (2019). Experimental investigation of multi-pass ECMAP process. *Transactions of the Indian Institute of Metals*, *72*(1), 239-244. https://doi.org/10.1007/s12666-018-1477-7